

ZIGGY: A HIGH-FLUX PARTICLE BEAM IMAGER

James Stevick
Kasper Research Team

I. Background and Motivation

As a member of the Kasper Research Team, I have been working under Dr. Kasper in Space Research, to develop a calibration system for an instrument boarding NASA's Europa mission. The mission will send nine advanced sensing instruments to one of Jupiter's moons, Europa, to determine if it contains conditions suitable for life. NASA's Galileo revealed strong evidence of an ocean below Europa's icy surface [1]. While Europa does not emit a magnetic field from an internal permanent dipole, Jupiter's massive time-varying magnetic field induces an electric field in Europa. This E-field causes a current to flow through Europa's interior ocean, which acts as a massive conductor, inducing its own magnetic field. The strength of this induced magnetic field is proportional to the salinity and depth of Europa's ocean as well as the thickness of Europa's icy surface [2]. Using multi-frequency electromagnetic sounding, ICEMAG's magnetometers will measure Europa's magnetic induction signal to determine information about Europa's ocean. Ionized plasma currents surrounding Europa bias the magnetic induction signal, requiring a Plasma Instrument for Magnetic Sounding (PIMS – See Appendix C1 and C2) to measure these plasma currents and correct for their bias. Particle accelerators in the Space Research Building fire lithium ions and electrons to calibrate PIMS. These particle accelerators must be calibrated themselves to ensure accuracy, precision, and strength in their particle beams (See Appendix C3 and C4). We have designed ZIGGY to accomplish this goal, measuring the location and spot size of the particle beam in real time, to calibrate the particle accelerator.

II. Introduction

In order to build the necessary calibration system, we implemented a wedge-strip-zigzag configuration of anodes for detecting particles [3]. Essentially, the particle beam from the accelerator hits three anodes on our sensor and the resulting currents are amplified and measured. Mathematical equations compute the location and spread of the particle beam based on the measured current magnitudes. Software translates real-time current data to incident location and spot-size of the beam, along with a user-friendly visualization and a graphical user interface for control.

III. Electrical Design

The wedge-strip-zigzag (WSZ) configuration, described by C. Martin et al., mathematically computes the location and spot-size of the particle beam. Figure 1a is a simplified version of the sensor, demonstrating how the wedges (W), strips (S), and zig-zag (Z) are configured. Picturing the image as a Cartesian coordinate system, strips vary linearly along x-axis, gaining width in the positive-x direction. Wedges vary linearly along the y-axis, beginning with a sharp point, and gaining width in the positive-y direction. The zig-zag is consistent over the whole sensor and proportional to the spot size of the incident beam. The real sensor uses many micron-scale wedges and strips, as depicted in Figure 1b. Equations 1a-1c describe how the X position, Y position, and Spot-size are determined from currents W,S, and Z.

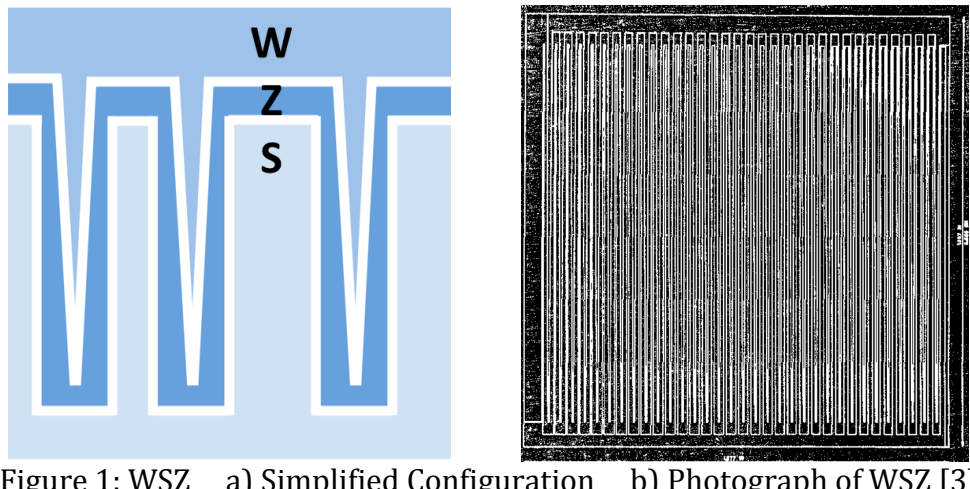


Figure 1: WSZ a) Simplified Configuration b) Photograph of WSZ [3]

$$X = \frac{2S}{W + S + Z} \quad Y = \frac{2W}{W + S + Z} \quad \text{Spot Size} = \frac{k(Z)}{W + S + Z}$$

Equation 1a, 1b, 1c: Position and Spot Size Equations [3]

Each of these three anodes conduct current through dual-stage operational amplifiers for a large range of measured input currents. Figure 2 depicts a flow chart of the currents with each shade of blue on the large square “WSZ” representing an anode, resulting in a low and high gain for each anode: Wedge, Strip, and Zig-Zag. Additionally, four calibration squares, shown in red, sit on each edge of WSZ with single-stage gain in order to center the particle beam. This is accomplished by balancing the voltages C_1 through C_4 . The design comprises 7 current inputs and 10 voltage outputs due to the current-to-voltage converting circuitry surrounding the inverting operational amplifiers.

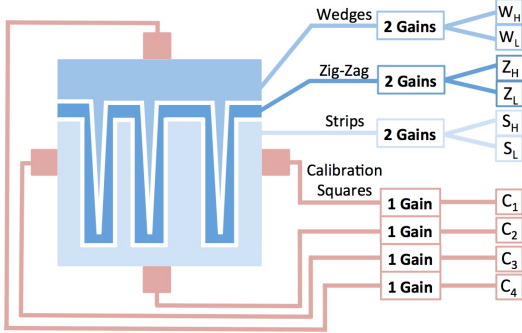


Figure 2: WSZ Current Flow Diagram

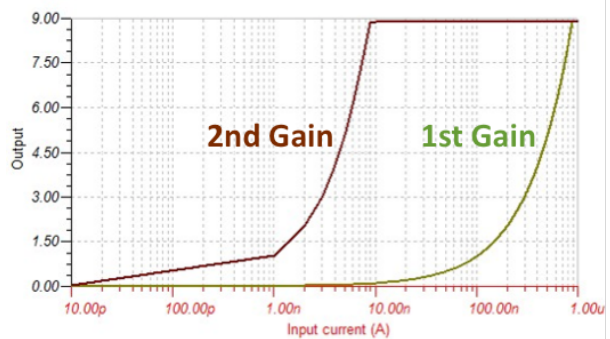


Figure 3: Graph of Dual Stage Amplification

1. Sensor Requirements

The project requirements included measuring currents from 10pA to $1\mu\text{A}$. Our first stage of gain converts current to voltage and amplifies by a factor of 10 million, providing suitable measurements for currents ranging from 10nA to $1\mu\text{A}$. Our second stage of gain, amplifies the 1st output voltage by a factor of 100, providing suitable measurements for lower currents ranging from 10 pA to 10nA . Since the output from the second gain is effectively 1 billion, it measures the lowest currents and consequently saturates quickly. Figure 3 demonstrates this effect with a semilogarithmic plot of voltage as a function of the large input range of the sensor. The operational amplifiers, powered by $\pm 10\text{V}$ rails, saturate around 9V. For the second stage gain, this corresponds to an input current of about 10nA , as shown where the 2nd gain plateaus in Figure 3.

2. Component Selection

For the low-gain operational amplifier, we chose an expensive OPA128 due to its extremely low input bias current of 75fA . The bias current becomes amplified along with the input current, so it is best to have a low current bias relative to our lowest input current of 10pA . The supplemental RC circuit, simplified in Figure 4a, offers a gain of R_1 (in our case $10\text{M}\Omega$) with a capacitor of 100nF . For the high gain, having already greatly amplified the signal, the bias currents and voltage offsets were less of a concern. We chose an OPA137 with a supplemental RC circuit simplified in Figure 4b. The resulting gain, using $100\text{k}\Omega$ and $1\text{k}\Omega$ resistors, is $\frac{R_2+R_3}{R_3} = \frac{100+1}{1} \approx 100$, supplemented by a capacitance of 120nF . For the calibration squares, we used OPA2137 (essentially two OPA137s in one package) with two stages of gain following the same circuitry described above, barring a 1nF capacitor in the RC circuit of the first gain. Here, we only care to balance the voltage outputs, so we only output the second gain. To validate the gain circuitry, we compared output signals from injected currents to simulations carried out on Altium Designer software. Graphs of these tests are described in the results section.

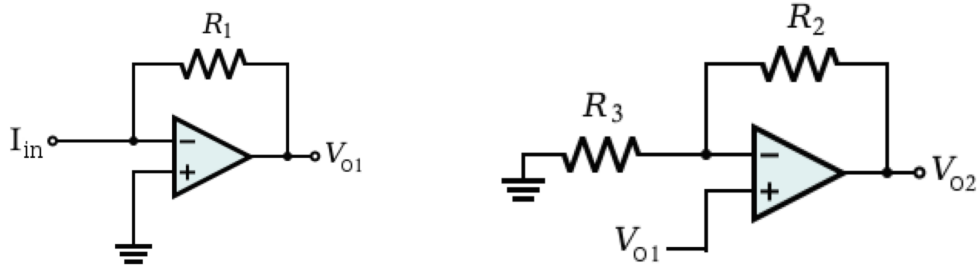


Figure 4: Inverting Operation Amplifier Circuits a) 1st Gain b) 2nd Gain

In order to reduce parasitic capacitance from noise in the circuitry or power supplies, we incorporated bypass capacitors. Although our system runs in a steady state, effectively dealing with direct current, we took extra precautions for transients. The circuit includes small and large bypass capacitors placed strategically to account for high and low frequency noise from power supplies and capacitive coupling between components.

3. Schematic & PCB Design

We began creating our schematic on Altium with 10 operation amplifiers, 21 resistors, 30 capacitors, and a 15-pin D-subminiature to provide routs for ground, power supplies, and output voltages (See Appendix A). Altium provides conversion and linked updating to its PCB Design software. In Altium PCB Designer, we began developing a 3-layer PCB, with through-hole components, and a fully grounded middle layer for maximum grounding area—this provides low resistance and means for quickly dispersing charge [4]. The 3-anode WSZ sensor was designed on AutoCAD as a .dwg file, imported onto Altium PCB Designer where it existed simply as a set of lines delineating the separation between the 3 anodes. This can be seen in a rendering of SWZ in our PCB design in Figure 5b below. By pouring a copper layer over the drawing and setting the lines of the drawing as no-pour restriction zones with a width of 5 thousandths of an inch, we effectively created the anode design with adjustable separation distances.

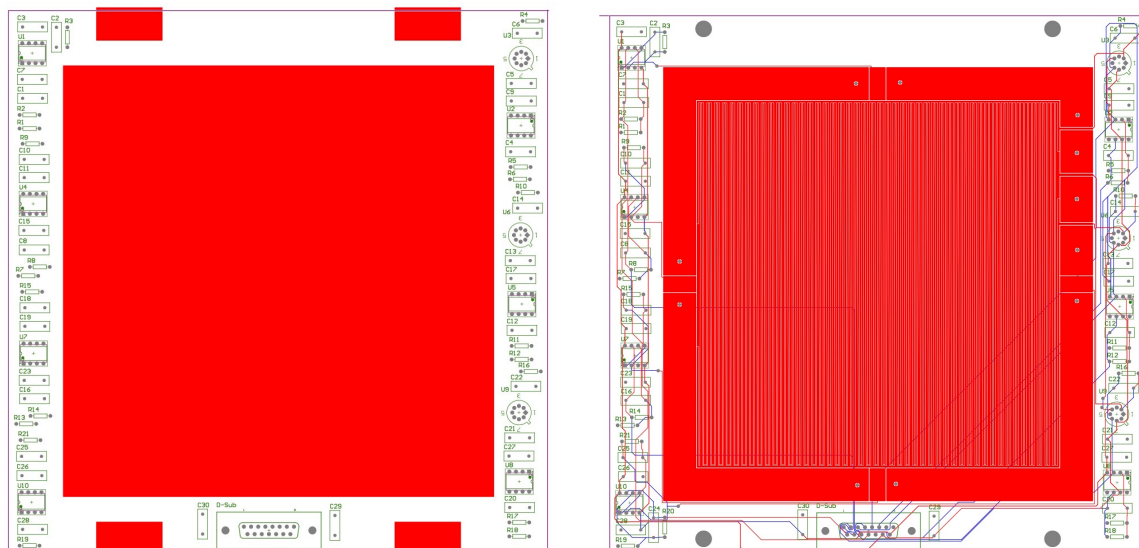


Figure 5: ZIGGY on Altium Designer a) PCB with Components and Restricted Zones b) Fully Routed PCB with ZIGGY

After the WSZ portion of ZIGGY had been imported and centered, we laid down the components and placed them in non-restricted areas. Figure 5a shows red squares where components and routing cannot occur due to obstructing functions. The large red square in the center covers the WSZ sensor, while the smaller red squares section off space for mounting screws, which can be seen as dark circles in Figure 5b. We carefully auto-routed as many connections as possible, automatically avoiding the red areas as shown in Figure 5b, a larger version of which can be found in Appendix B. With only two layers for routing, and hundreds of pin connections, we inevitably ran into instances of overlapping wires resulting in a short circuit. We implemented through-hole vias accordingly to jump wires or switch between layers. In Appendix B, four calibration squares (more like rectangles) sit in the center of each edge, sending signals to the four dual-stage op-amps lining the left side. The three anodes exit SWZ at the upper right side, sending signals directly to three round op-amps lining the right side, along with their associated circuitry and additional op-amps. At the bottom of the PCB sits the D-sub and two low frequency bypass capacitors. Figure 6a shows a 3-D rendering of our PCB on Altium, where a student in CEE575 may also notice 2D aliasing.

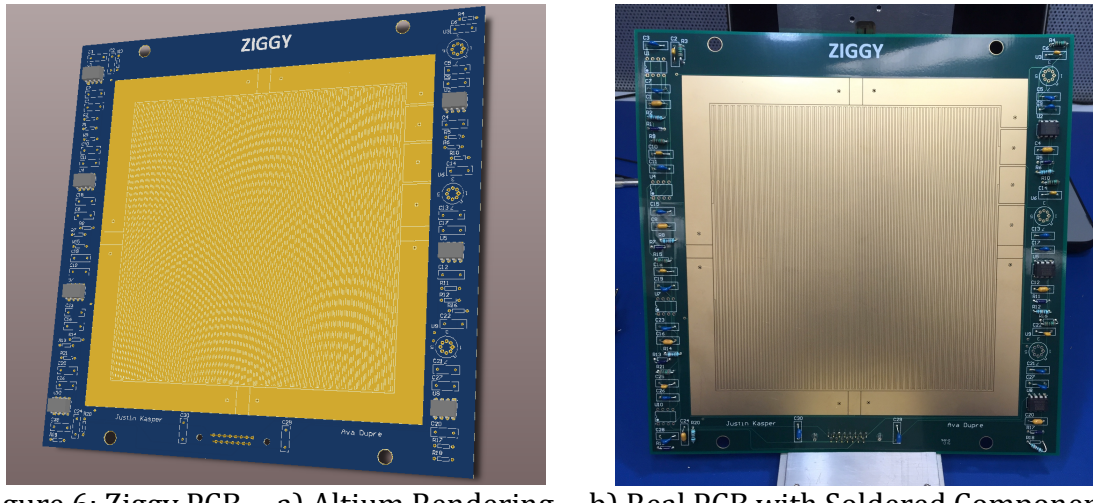


Figure 6: Ziggy PCB a) Altium Rendering b) Real PCB with Soldered Components

The intricacies of ZIGGY are more clearly visible in Figure 6b. The golden copper surface of the SWZ sensor shows just how thin and close together the strips and wedges lie. The four rectangular calibration squares and three anode leads border the SWZ square, along with grounded copper completing the square border. The visible dots are through-hole vias connecting the grounded central layer to the grounded copper pours on the surface. After reviewing many software warnings and errors, adjusting hole sizes, changing wire thicknesses, and searching through the many turns of SWZ for any disconnections, we sent our PCB design to Dr. Rogaki and Dr. Rizor, senior Electrical Engineers at University of Michigan. They approved our design, and created Gerber files to be sent off for production of our PCB. Upon arrival, we soldered 197 points to completely secure all components to the PCB. Figure 6b shows the real PCB with majority of the components soldered.

IV. Mechanical Design

We designed the mechanical housing on SOLIDWORKS, documented manufacturing drawings and specification sheets, and finally manufactured the parts. The baseplate contains a grid of tapped holes at 2" spacing to mount to the vacuum chamber, as shown in Appendix D1. This allows us to adjust the distance from the sensor to the particle accelerator. The box to secure and insulate ZIGGY is manufactured from a monolithic slab of Aluminum, which serves to resist vibration. The back braces shown in Appendix D2 add stability. Blocks of Ultem (vacuum-compatible electrical-insulating material) provide step-like levels of mounting for the PCB and two layers of mesh shielding. These components can be found in yellow in Appendix D3.

1. Mesh Grid E-Field

The function of the mesh grids, known as the Suppressor Grid and the Grounding Grid, is two-fold. Two mesh grids sit between ZIGGY and the particle beam with an adjustable voltage potential difference. The electric field created by the potential between the two mesh grids filters particles by energy and suppresses particle bounce to reduce noise. Appendix D3 shows a grey plate representing ZIGGY, with the frame of the Grounding Grid secured to the yellow blocks of Ultem. The Grounding Grid attaches to this frame, providing chassis grounding to the system. Appendix D4 shows the wider, higher-voltage frame to the Suppressor Grid, which also serves to shield the components from wayward charged particles. The grids are not shown in these renderings, but Figure 7b shows the actual mesh grid. Figure 7a shows how the outer frame sits above ZIGGY, shielding the electrical components of ZIGGY, revealing only the SWZ and the surrounding calibration squares.

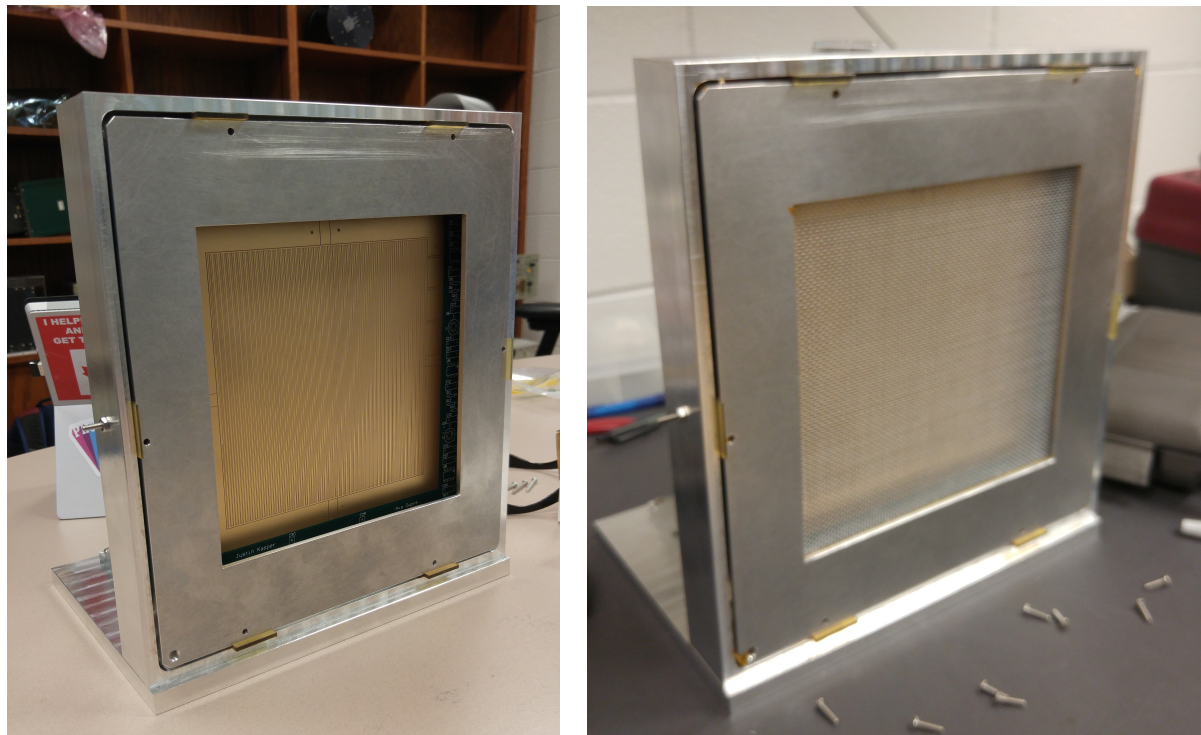


Figure 7: Manufactured ZIGGY a) Without Mesh b) With Mesh

V. Data Processing

Our program, written in python, translates sensor output voltages to a visual representation of beam position and spread. An NI-DAQ continuously collects data and our program runs it through data filtration and positioning algorithms to provide real-time visualization. Appendix E2 shows the software architecture, modularized into several components including a random data generator for testing, voltage conversion system, user interface, real-time display, and a calibration system. The calibration system acts like a tare button on a scale, measuring output voltages when the particle accelerator is off, and correcting for its bias. Appendix E1 depicts a flow chart of data from the particle beam to the real-time display. The NI-DAQ sends inputs through the calibration and filtration systems, into the positioning algorithm, and outputs to a real-time display. Appendix E3 shows our user interface. One can view the position in Cartesian coordinates as well as the beam spot-size displayed in concentric circles. Centering the beam requires balanced currents on all four of the calibration squares, which turn colors based on their relative values. Red conveys a high current, green conveys a low current, and yellow means the currents are balanced.

VI. Results

Given limited access to the particle accelerator, we have resorted to injecting currents to ensure a properly functioning circuit board, examine the gain characteristics, and test the user interface. The user interface works as described above, ensuring a properly functioning program for real-time data collection and processing. This was tested both with randomly generated data through the program as well as injecting currents and collecting data with an NI-DAQ. We were able to test the gain circuitry by injecting currents and found that they approximated their theoretical characteristics with slight bias, as operational amplifiers have naturally drifting offsets.

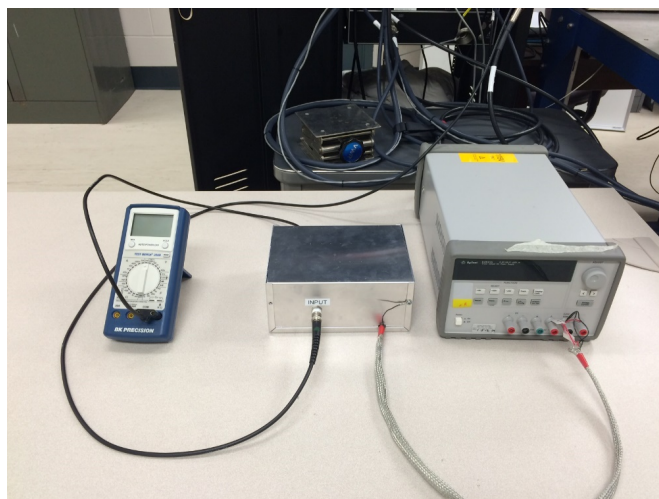


Figure 8: Current Generator Testing System

1. Calibration Squares

We began testing the calibration squares by injecting currents to test their gain circuitry. Figure 8 shows our current generator supplying current to a metal box, which

encapsulates our circuit, and outputs to a multi-meter for measurement. We recorded output values from input currents and found appropriate values within a margin of offset error. This is sufficient testing for the calibration squares, as our goal is to center the particle beam to a reasonable level of accuracy. As long as all four operational amplifiers circuits output gain characteristics with a reasonably small offset, they will sufficiently balance to center our particle beam within our desired error limits.

2. WSZ Sensor

We began testing the WSZ sensor with the current supply as well, checking that the gain circuitry follows our theoretical characteristics within margins of error. Collecting data with an NI-DAQ, we plotted the gain characteristics for the low and high gain (see Figure 9). The curves follow our desired characteristics, and confirm proper functioning of our PCB. With access to the particle accelerator, we centered a beam of electrons on the sensor, and measured the output voltages from the single-stage gain of the WSZ circuitry. Figure 10 shows the output characteristics from the charged particle beam relative to simulated data. The two plots reveal a very close correlation between the simulated gain characteristics and actual output voltages from charged particles.

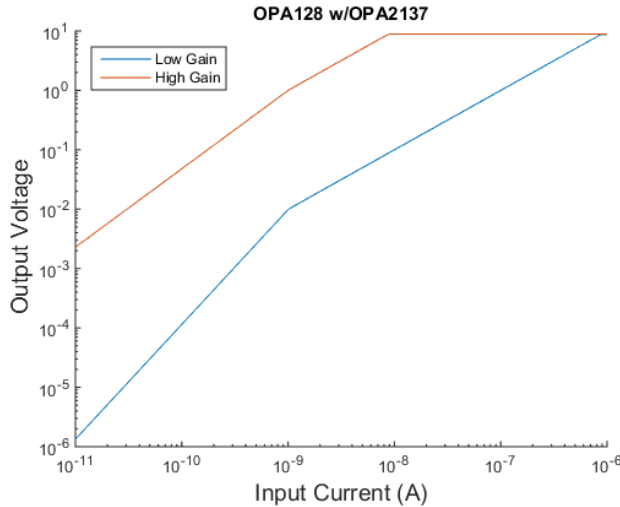


Figure 9: Low and High Gain of SWZ Circuitry

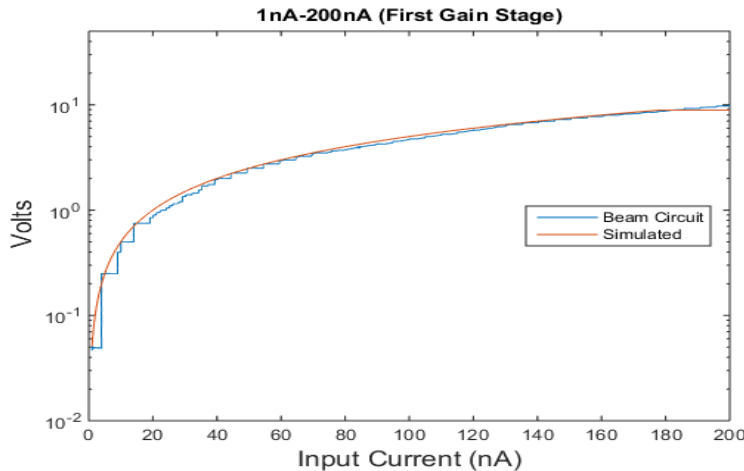


Figure 10: Low Gain Simulation vs. Beam Supply

VII. Discussion

Our next steps are to fully calibrate our PCB using a current generator on the remaining operation amplifiers to get accurate characteristics of the gain systems. Then we will test the full sensor in the vacuum chamber and fire both lithium ions and electrons at ZIGGY. Our software will properly center the particle beam and correct for any naturally occurring voltage offsets, allowing us to calibrate and control the location and spot-size of the particle beam.

We hope to decrease the size of ZIGGY over the following semester in order to implement a system of higher resolution. ZIGGY 2.0 will comprise sixty-four WSZ sensors for a 64-pixel system. This will require additional circuitry, a new mechanical housing, and updated modules for the data filtration and user interface system.

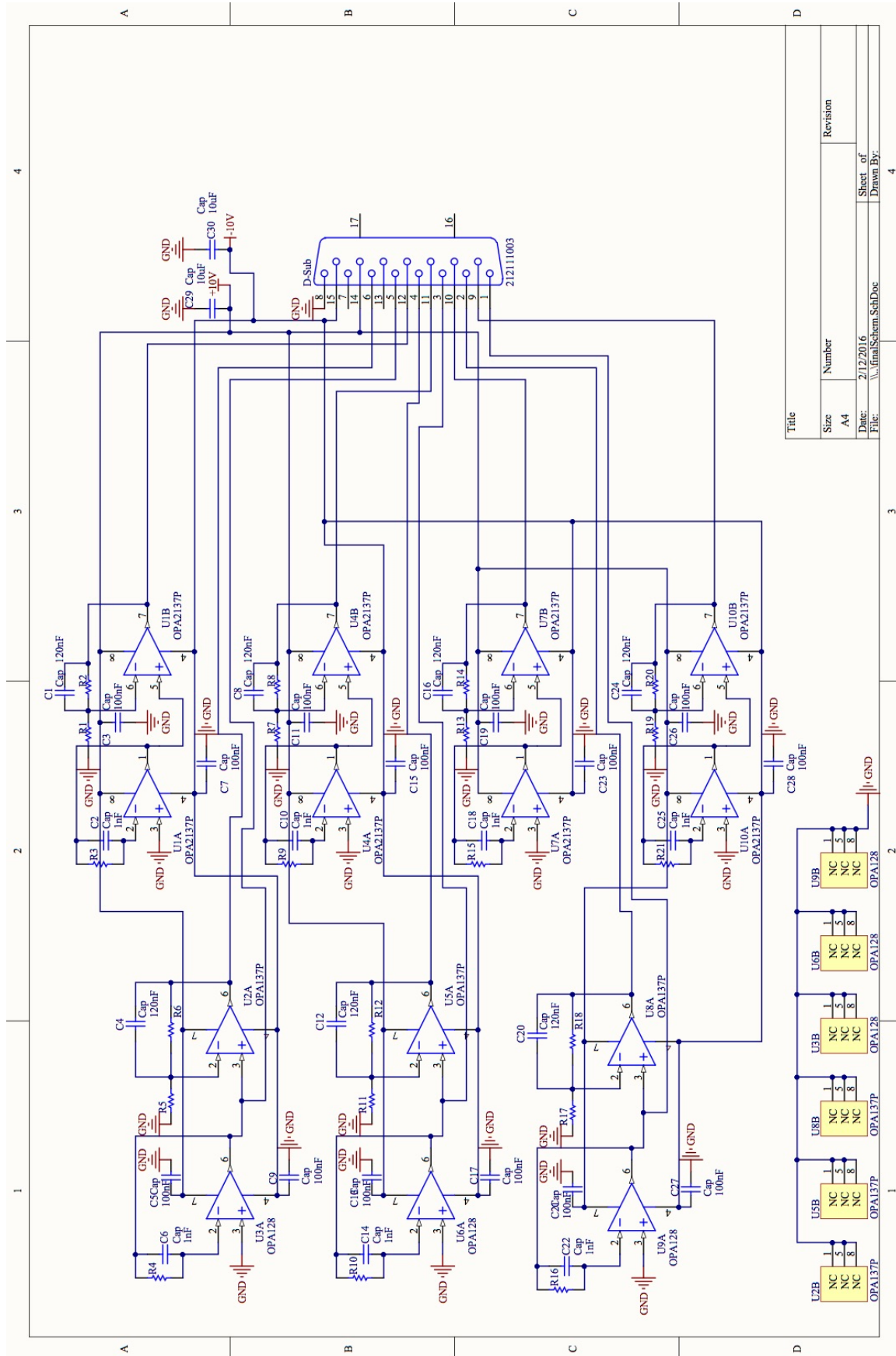
As PIMS measures plasma currents—chaotically surrounding Europa—with more precision, the magnetometer will provide a more precise magnetic induction signal from the current flowing through Europa's ocean. As we increase the accuracy of the signal, we gain knowledge about Europa's ocean, bringing us closer to evaluating Europa's ability to contain life.

References

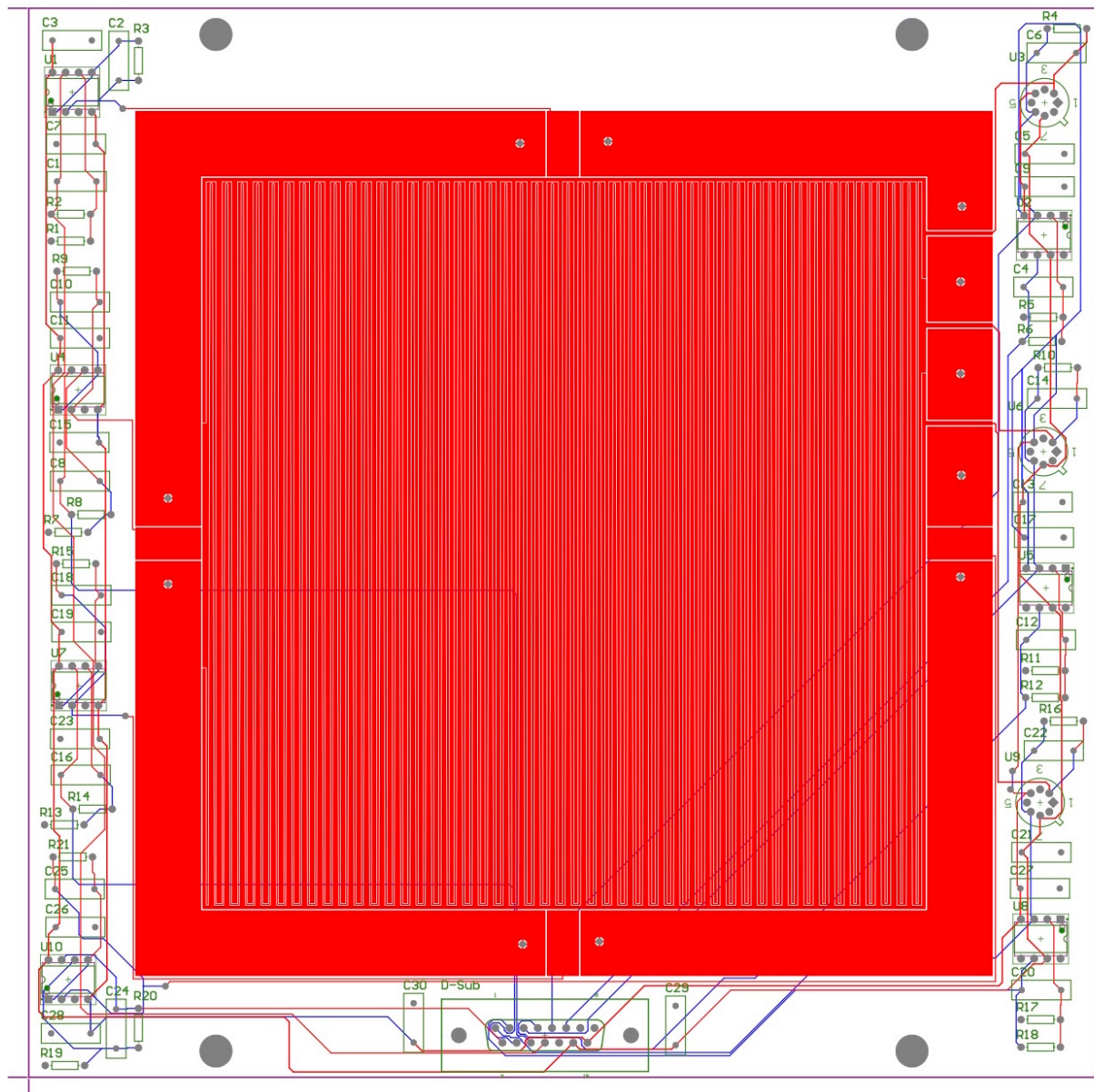
- [1] Dyches, Preston and Dwayne Brown, "NASA's Europa Mission Begins with Selection of Science Instruments", May 26, 2015,
<<http://www.jpl.nasa.gov/news/news.php?feature=4598>>
- [2] Phillips, Cynthia, *Magnetic Fields and Water on Europa*, SETI Institute, February 26, 2004, <<http://archive.seti.org/news/features/magnetic-fields-europa.php>>
- [3] C. Martin et al., *Wedge-and-Strip Anodes for Centroid-Finding Position-Sensitive Photon and Particle Detectors*, Space Sciences Laboratory, February 9, 1981
- [4] Mancini, Ron, *Op Amps For Everyone: Design Reference*, Texas Instruments, August 2002, ch. 17, pg. 353
- [5] Fainberg, E. B., *Electromagnetic Induction in the World Ocean*, Geophysical Surveys, 1980

Appendices

Appendix A: Schematic for Printed Circuit Board ZIGGY

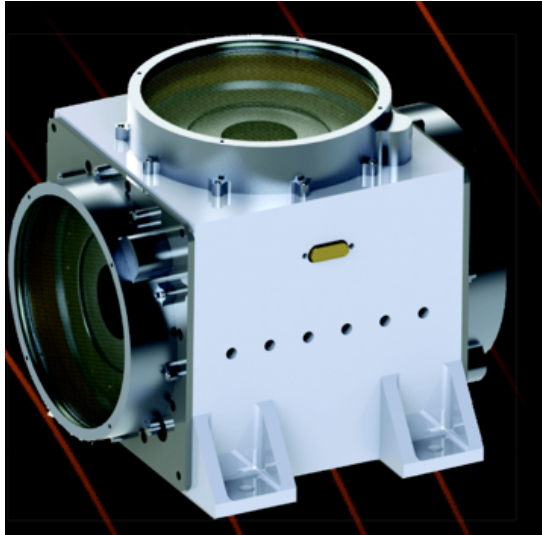


Appendix B: Fully Routed ZIGGY PCB on Altium Designer

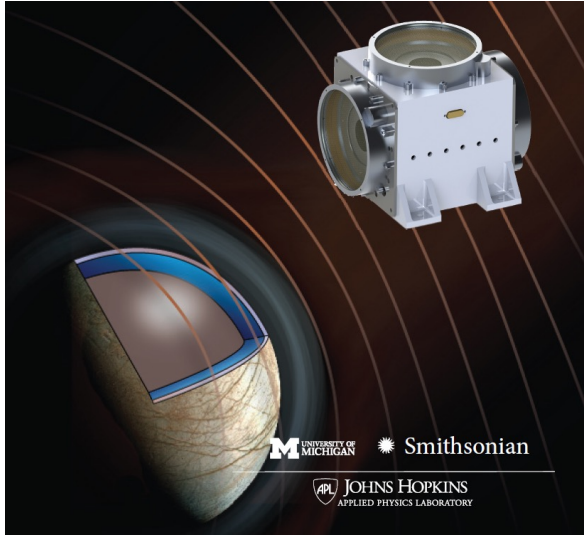


Appendix C: PIMS and Testing Chamber

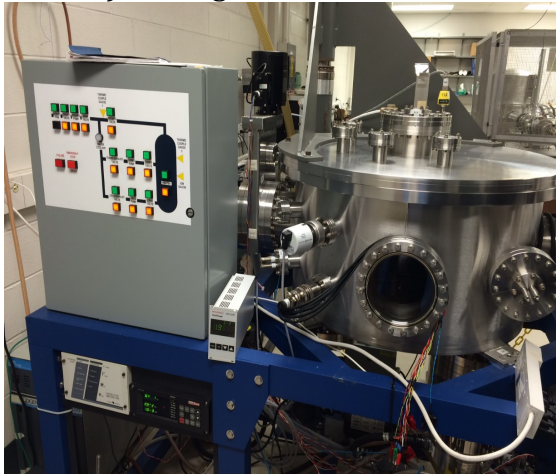
1) PIMS Instrument



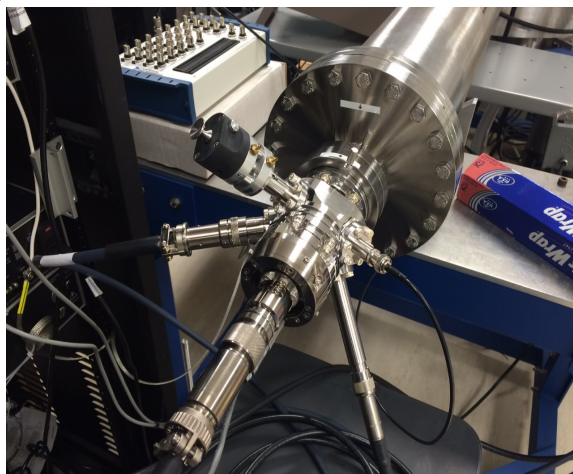
2) PIMS in Europa's Magnetic Fields



3) Testing Vacuum Chamber

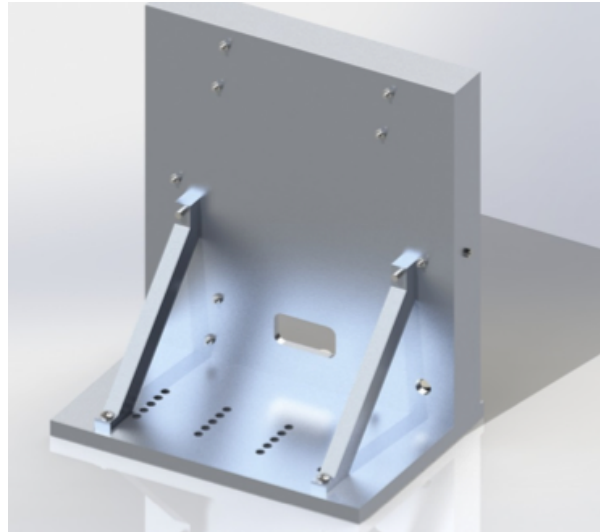


4) Particle Accelerator Attached to Chamber

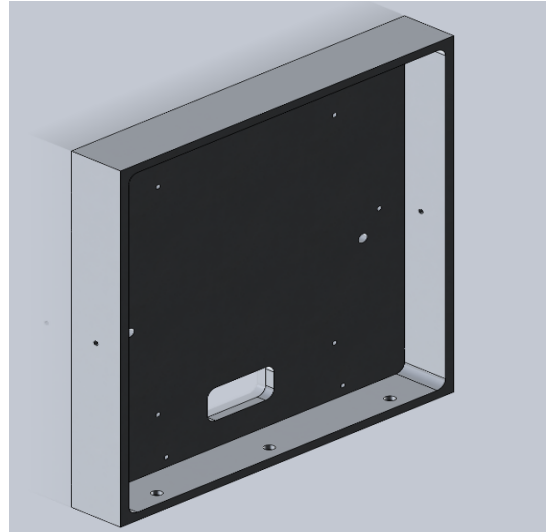


Appendix D: Mechanical Housing (SOLIDWORKS)

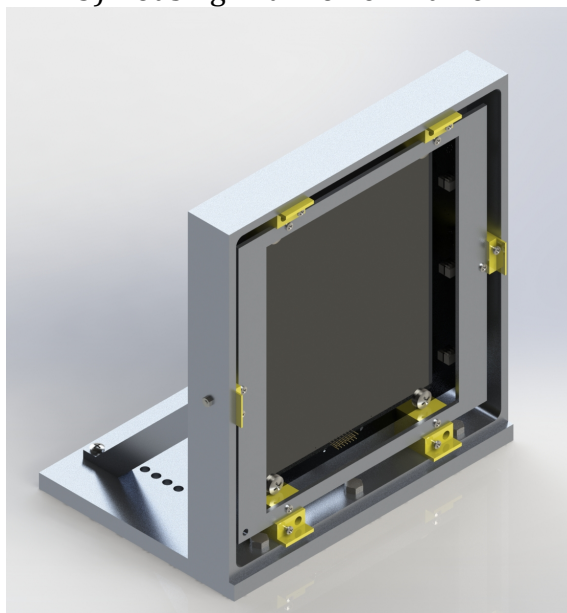
1) Housing Support and Attachment



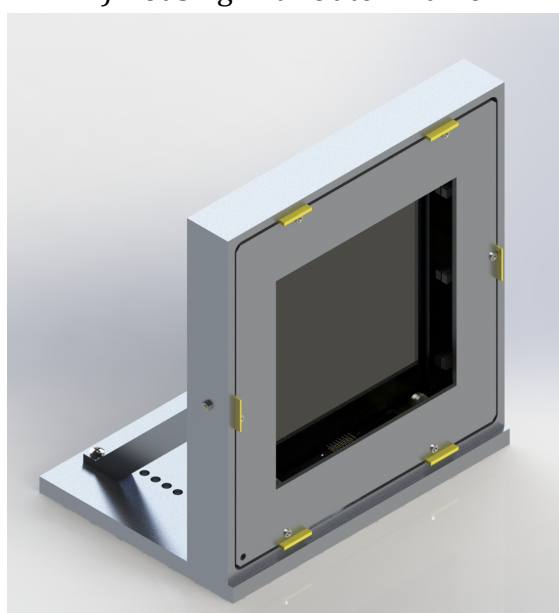
2) Monolithic Aluminum Milled Box



3) Housing with Lower Frame

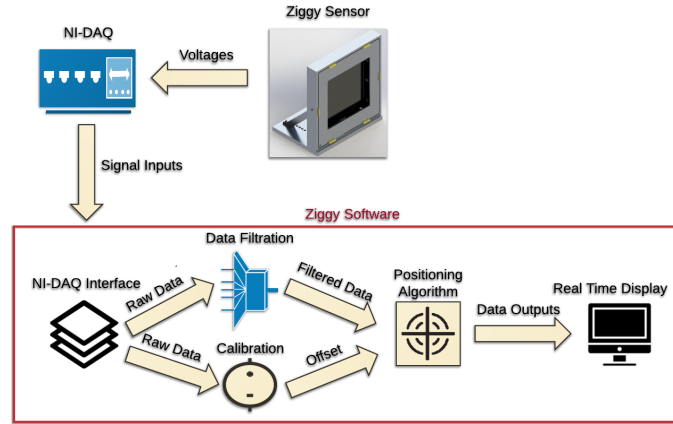


4) Housing with Outer Frame

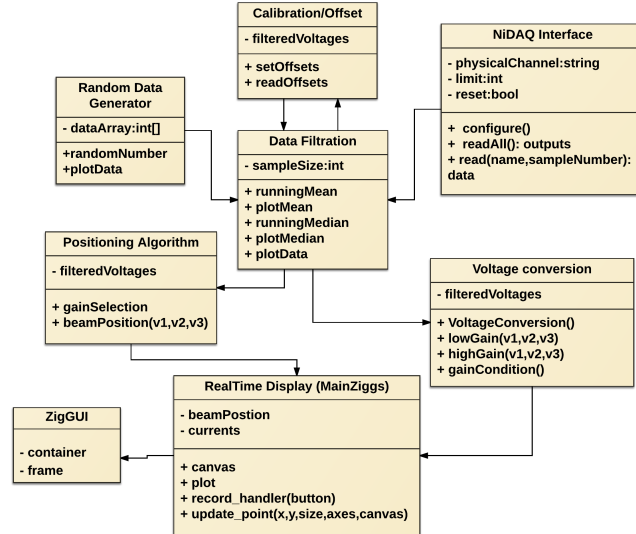


Appendix E: Programming Diagrams

1) Flow Chart from ZIGGY to GUI



2) Programming Modules



3) User Interface Real-Time Display

